

Dynamics of a degenerate Fermi gas in a one-dimensional optical lattice coupled to a cavity

Qing Sun,¹ Xing-Hua Hu,¹ An-Chun Ji,^{2,*} and W. M. Liu¹

¹Beijing National Laboratory for Condensed Matter Physics, Institute of Physics, Chinese Academy of Sciences, Beijing 100190, China

²Center of Theoretical Physics, Department of Physics, Capital Normal University, Beijing 100048, China

(Received 30 November 2010; published 6 April 2011)

We systematically study the dynamics of a one-dimensional degenerate Fermi gas in an optical-lattice potential coupled to a single-mode cavity field. We derive an effective model to study the nonperturbative effect caused by the cavity field. Our numerical results show that due to the addition of the optical-lattice potential, the system undergoes second-order transition to a bistable density-wave steady state, where the atoms form a density wave and the cavity field is bistable. In addition, the coherent oscillating behavior of the cavity photon number can be observed. We also present a feasible experimental protocol to realize these phenomena, which may be beneficial for future quantum-information applications.

DOI: [10.1103/PhysRevA.83.043606](https://doi.org/10.1103/PhysRevA.83.043606)

PACS number(s): 03.75.Ss, 37.10.Jk, 42.50.Pq, 42.65.Pc

I. INTRODUCTION

With the realization of strong coupling of Bose-Einstein condensates (BEC) with an electromagnetic-field mode of a high-finesse cavity [1,2], the cavity quantum electrodynamics (QED) combined with cold atom physics has attracted great experimental and theoretical interest, and achieved considerable advances. For example, by using the cavity QED method, new approaches to extract the quantum-state properties of ultracold atoms have been proposed [3,4], and the superfluid–Mott-insulator transition of the cold atoms in quantum optical-lattice potential [5] has been studied in Ref. [6]. Further, recent experiments [7,8] have realized optomechanics in which cold atoms assemble in a cavity, where either the side-mode excitations of a bosonic condensate [7] or the vibrational motion of cold thermal atoms [8] can serve as a mechanical oscillator. Such cavity-optomechanical analogs have also been extended to the degenerate Fermi gas [9].

One of the remarkable characteristics of these atom-cavity systems is the intrinsic nonlinearity. In the large detuning limit, the dispersive nature of the atom-photon interaction yields a dipole potential (or optical-lattice potential) to the atoms, and meanwhile the atomic motion shifts the cavity-mode frequency. Because of the interdependence between the atomic state and the cavity field, the atom-cavity system is determined self-consistently. This nonlinear interaction has been observed in Ref. [8], and could lead to the complex dynamics of a Bose-Einstein condensate in a cavity [10–13], especially the self-organized superradiant phase transition of atoms in transversally pumped cavities [14–18]. An intriguing phenomenon associated with the nonlinearity is the possible emergence of optical bistability [19], which has been observed in different atom-cavity systems [8,20,21].

However, these works did not fully consider the influence of possible external potential, especially the optical-lattice potential. The optical-lattice potential is not only a powerful tool to control the cold atoms with high tunability, but also a platform to study the condensed matter physics with cold atoms [22]. Actually, the technology of adding optical lattice to the cavity-atom system has been readily applied

in recent experiments [2], where the important effect of the optical-lattice potential is the emergence of the band structure. However, how the band structure affects the coupled dynamics of the atom-cavity system has not been studied.

In this paper, we consider a system consisting of spin-polarized ultracold Fermi atoms in a high- Q optical cavity driven by a laser field as illustrated in Fig. 1. Compared with the previous work [9], we add a strong optical-lattice potential along the axis to form a one-dimensional (1D) lattice gas. We derive an effective spin model to describe this atom-cavity system for a small cavity photon number limit. Then we determine the atomic state together with the quantized light field self-consistently. We find that optical bistability and coherent oscillation of the intracavity photon number can also be observed in this atom-cavity system, and the atoms are in a density wave (DW) state, which is not reported in the previous works.

This paper is organized as follows. In Sec. II, we derive an effective model to describe this atom-cavity system. Based on the model, we study the coupled dynamics, including the possible steady state in Sec. III A and the dynamical evolution in Sec. III B. Some discussion on experiments is presented in Sec. IV. Finally, we give a summary in Sec. V.

II. THE MODEL

We start by considering the single-particle Hamiltonian [6] of a single-mode Fabry-Pérot cavity with cold atoms, which interact with the cavity mode dispersively in a far-detuning limit:

$$\hat{H}_0 = \frac{\hat{P}^2}{2m} + V_{\text{op}}(K_o \hat{X}) + \hbar U_0 \cos^2(K_c \hat{X}) \hat{a}^\dagger \hat{a} - \Delta_c \hat{a}^\dagger \hat{a} - i\hbar\eta(\hat{a} - \hat{a}^\dagger), \quad (1)$$

where \hat{a}^\dagger and \hat{a} are the creation and annihilation operators of the cavity mode with wave vector K_c , and \hat{P} , \hat{X} , and m are the momentum, position, and mass of atoms, respectively. η is the cavity-pumping strength at frequency ω_p and $\Delta_c = \omega_p - \omega_c$ is the cavity-pumping detuning. $V_{\text{op}}(\hat{X}) = U \cos^2(K_o \hat{X})$ is a classical optical potential independent of atoms with wave vector K_o and strength U . The atom dipole transition is far off resonance from the cavity mode, and induces a dipole potential

*andrewjee@sina.com

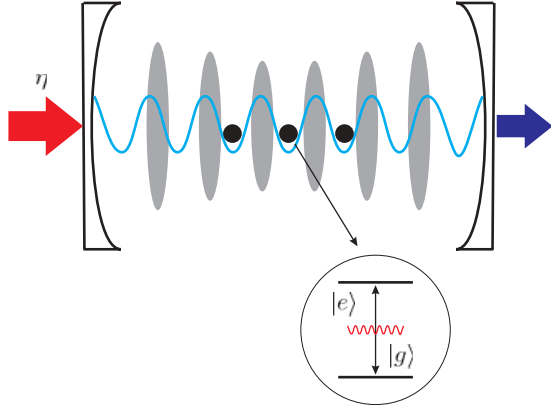


FIG. 1. (Color online) Sketch of setup: N_a ultracold spin-polarized Fermi atoms are trapped in a Fabry-Pérot cavity. A 1D classical optical-lattice potential (blue line) along the cavity axis is engineered to confine the atoms into a lattice gas. The cavity field, which couples to the atomic internal energy levels $|e\rangle$ and $|g\rangle$, is pumped by a laser beam with strength η .

on the atoms with single-photon potential depth $U_0 = g^2/\Delta_a$, where $\Delta_a = \omega_p - \omega_a$ is the atom-pumping detuning and g is the single-photon Rabi frequency.

In actual experiments, an additional weak, isotropic external harmonic potential (e.g., a magnetic or optical trap) is needed to trap the atoms from escaping. This confinement brings an energy offset of each lattice site and leads to an effective local site-dependent chemical potential $\mu(i) = \mu + \frac{1}{2}m\omega_r^2 x_i^2$ for the harmonic case. However, for a lattice with 100 sites along a single direction, the Zeeman energy for atoms in different sites varies from $10^{-5}E_r$ to $10^{-2}E_r$, which is much smaller than the tunneling energy. Thus, this additional harmonic potential can be ignored, and we only consider the homogeneous case in the following discussion. Moreover, we also drop the constant part of the chemical potential, which does not affect the dynamical behavior of this system.

In the following, we assume that the quantum-dipole potential is much smaller than the classical optical-lattice potential, which can be controlled by tuning the strength of the cavity pumping or the external optical potential. Thus we can expand the atomic field operator as $\hat{\Psi}(x) = \sum_i \hat{f}_i w(x - x_i)$, where $w(x - x_i)$ and \hat{f}_i are the lowest-band Wannier function and fermion annihilation operator at site i of the lattice potential, respectively. At low temperature, this is valid when the band gap Δ_{BG} satisfies $\Delta_{\text{BG}} \gg kT, U_0 \bar{n}$. In the tight-binding approximation and within the momentum representation, the atomic Hamiltonian [first three terms in the Hamiltonian given by (1)] is written as

$$\hat{H}_a = \sum_k (\varepsilon_k - \mu) \hat{f}_k^\dagger \hat{f}_k + \frac{U_0}{4} \hat{n} \sum_k (\hat{f}_k^\dagger \hat{f}_{k+2K_c} + \text{H.c.}), \quad (2)$$

where $\varepsilon_k = -2t \cos k$ with the nearest-neighbor atomic hopping amplitude $t = \int w^*(x - x_j) \left(-\frac{\nabla^2}{2m_a}\right) w(x - x_i) dx$. Here, the overlap integral of the Wannier function only depends on the optical-lattice potential, and the quantum-dipole potential just shifts the chemical potential $\mu \rightarrow \mu + U_0 \bar{n}/2$ and induces a momentum transfer of $Q = 2K_c$ in the atomic state.

The Hamiltonian given by (2) is a good starting point to describe the coupled dynamics of single-mode cavity QED, interacting with cold atoms dispersively. Without an optical-lattice potential, previous experimental [7] and theoretical [9] studies show that both Bose and Fermi gases can behave as a harmonic-oscillator coupling to a cavity mode in the weak excitation limit. However, when we turn on a strong optical-lattice potential to confine the atoms, not only is the dispersion relation replaced by ε_k , but also the collective behavior of the atoms could be qualitatively changed and a density wave state may appear. Here, the cavity field induces a quantum-dipole potential, which is actually a weak-period potential [5], and the atomic wave functions diffracted by this potential interfere with each other. Once this dipole potential is commensurate with the optical lattice, a density wave state forms. To show this scenario, in the following we consider the case of $K_o = 2K_c$, without losing generality, where the atomic momentum transfer induced by the cavity field is $Q = 2K_c = \pi$.

In comparison with previous works [7,9], where the atomic operator is expanded with the plane-wave basis and further truncation of the atomic Hilbert space is needed to determine the dynamics in the limit of small photon number, here we deal with the system in the lowest Bloch band and the Hamiltonian given by (2) can be solved without further approximations. As stated above, the cavity field only mixes momentum k and $k + \pi$ states of atoms, which can be effectively considered as a system of many “two-level” structures interacting with a single cavity mode. By introducing a two-component spinor $\varphi(k) = (\hat{f}_k, \hat{f}_{k+\pi})^T$, we can rewrite the atomic Hamiltonian (2) as

$$\hat{H}_a = \sum_k' \varepsilon_k \hat{\sigma}_k^z + \frac{U_0}{2} \hat{n} \sum_k \hat{\sigma}_k^x, \quad (3)$$

where $\hat{\sigma}_k^x, \hat{\sigma}_k^z$ are Pauli matrices satisfying $\epsilon_{\alpha\beta\gamma} \hat{\sigma}^\alpha \hat{\sigma}^\beta = i \hat{\sigma}^\gamma$; $\alpha, \beta, \gamma = x, y, z$; and the summation of k is limited to the half of the first Brillouin zone. In the deviation of Eq. (3), we have used $\varepsilon_{k+\pi} = -\varepsilon_k$. This Hamiltonian can be seen as N_a noninteracting spins in an inhomogeneous external “magnetic field,” with the traverse field (spin quadratures) controlled by the cavity field.

III. DYNAMICS

Next, we determine the coupled dynamics of this atom-cavity system, with the corresponding Heisenberg equations of Eq. (2) given by

$$\begin{cases} \frac{d\hat{\sigma}_k^x}{dt} = -2\varepsilon_k \hat{\sigma}_k^y, \\ \frac{d\hat{\sigma}_k^y}{dt} = 2\varepsilon_k \hat{\sigma}_k^x - 2\left(\frac{U_0}{2} \hat{n} \hat{\sigma}_k^z\right), \\ \frac{d\hat{\sigma}_k^z}{dt} = 2\left(\frac{U_0}{2} \hat{n} \hat{\sigma}_k^y\right), \\ \frac{d\hat{a}}{dt} = -i(\bar{\Delta}_c + \frac{U_0}{2} \sum_k \hat{\sigma}_k^x) \hat{a} + \eta - \kappa \hat{a}, \end{cases} \quad (4)$$

where we have introduced the decay κ to describe the cavity dumping. In the following, we shall first consider the mean-field steady-state solution of the above Heisenberg equations, and then investigate the dynamical evolution of this coupled atom-cavity system.

A. Steady state: Bistable DW state

To get the mean-field steady-state solutions, we replace all the operators in Eq. (4) with their mean-field values $\langle \hat{O} \rangle$ and set all the time derivatives to be zeros, which yields

$$\begin{aligned} \langle \hat{\sigma}_k^y \rangle &= 0, \\ \langle \hat{\sigma}_k^z \rangle &= \frac{2\varepsilon_k}{U_0 \bar{n}} \langle \hat{\sigma}_k^x \rangle, \\ \langle \hat{a} \rangle &= \frac{\eta}{\kappa + i \left(\Delta + \frac{U_0}{2} \sum_k \langle \hat{\sigma}_k^x \rangle \right)}. \end{aligned}$$

Together with the normalization condition

$$\langle \hat{\sigma}_k^x \rangle^2 + \langle \hat{\sigma}_k^y \rangle^2 + \langle \hat{\sigma}_k^z \rangle^2 = \begin{cases} 1 & (\hat{n}_k + \hat{n}_{k+Q} = 1) \\ 0 & (\hat{n}_k + \hat{n}_{k+Q} = 0 \text{ or } 2), \end{cases} \quad (5)$$

the cavity field can be self-consistently determined as

$$\bar{n} = \frac{\eta^2}{\kappa^2 + \left(\bar{\Delta}_c + \frac{U_0}{2} \sum_k \frac{\bar{n}}{\sqrt{(2\varepsilon_k)^2 + U_0^2 \bar{n}^2}} \right)^2}. \quad (6)$$

The normalization condition (5) shows that only the single occupied state of the two-level structure contributes to the dynamics up to a trivial shift of cavity detuning $\bar{\Delta}_c$ scaled with atom number N_a . For Eq. (6), we find that there exist multiple solutions, which implies that optical bistability may occur. This is the unique character of such coupled atom-cavity systems. Further, our linear stability analysis confirms that the steady state is bistable. Now, we numerically solve Eq. (6) self-consistently and the results are shown in Fig. 2. In Fig. 2(a), we give the bistability curves of the steady-state mean intracavity photon number \bar{n} as a function of cavity detuning $\bar{\Delta}_c$ for fixed η/κ , and in Fig. 2(b), as a function of pumping strength η for fixed cavity detuning. The dashed line in Fig. 2 with negative slope is unstable, while the other regimes are stable. Such optical bistability arises from the intrinsic nonlinearity of the cavity QED with cold atom systems, which has been reported both in experiment [7] and theory [9].

To better understand the physics underlying the atom-cavity steady state, we replace the photon number operator \hat{n} in Eq. (2) with the temporary value \bar{n} and neglect the fluctuations, which is valid in a mean-field steady state. Then the atomic Hamiltonian is bilinear and can be diagonalized by introducing a set of Bogoliubov transformations,

$$\begin{aligned} \hat{f}_k &= \cos \theta_k \hat{b}_k + \sin \theta_k \hat{b}_{k+\pi}, \\ \hat{f}_{k+\pi} &= \cos \theta_k \hat{b}_{k+\pi} - \sin \theta_k \hat{b}_k, \end{aligned} \quad (7)$$

with the inverse transformation

$$\begin{aligned} \hat{b}_k &= \cos \theta_k \hat{f}_k - \sin \theta_k \hat{f}_{k+\pi}, \\ \hat{b}_{k+\pi} &= \cos \theta_k \hat{f}_{k+\pi} + \sin \theta_k \hat{f}_k, \end{aligned} \quad (8)$$

where θ_k satisfies $\tan(2\theta_k) = -U_0 \bar{n} / 2\varepsilon_k$. The Hamiltonian given by (2) now is diagonalized and can be written as $\hat{H}_a^{\text{diag}} = \sum_k \xi_k \hat{b}_k^\dagger \hat{b}_k + \text{const.}$ Here the energy spectrum

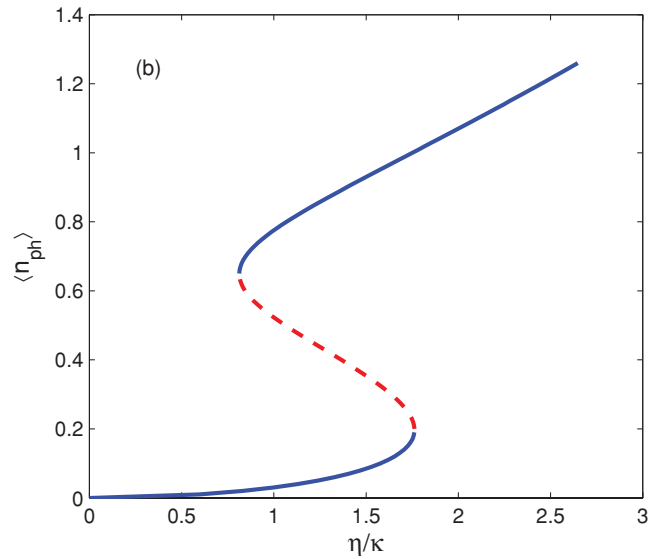
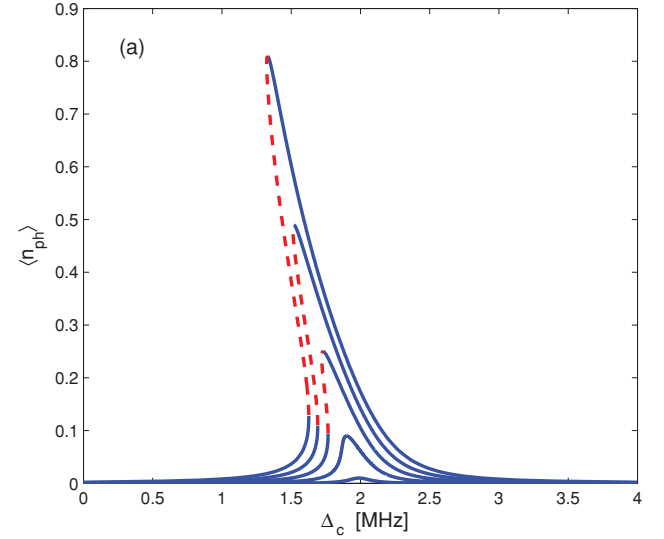


FIG. 2. (Color online) Steady-state intracavity photon number as a function of (a) pump-cavity detuning for (by increasing maxima) $\eta/\kappa = 0.1, 0.3, 0.5, 0.7, \text{ and } 0.9$; (b) pumping strength for $\Delta_c = 1.4$ MHz. Other parameters are chosen as $t/\kappa = 0.1$, $N_a = 200$, and $U_0 = 10$ kHz.

$\xi_k = \pm \sqrt{\varepsilon_k^2 + \Delta_g^2}$ with a gap $\Delta_g = U_0 \bar{n} / 2$ can be exactly determined self-consistently through

$$\Delta_g = \frac{U_0 \eta^2 / 2}{\kappa^2 + \left(\bar{\Delta}_c + \frac{U_0}{2} \sum_k \Delta_g / \sqrt{\varepsilon_k^2 + \Delta_g^2} \right)^2}. \quad (9)$$

Note that the quasiparticle introduced in Eq. (8) just describes a density wave state, where the atoms suffer a momentum transfer $\pm 2K_c$ due to the photon recoil by the off-resonance standing-wave field interference with each other. This DW instability occurs at an arbitrary, nonvanishing cavity-field amplitude.

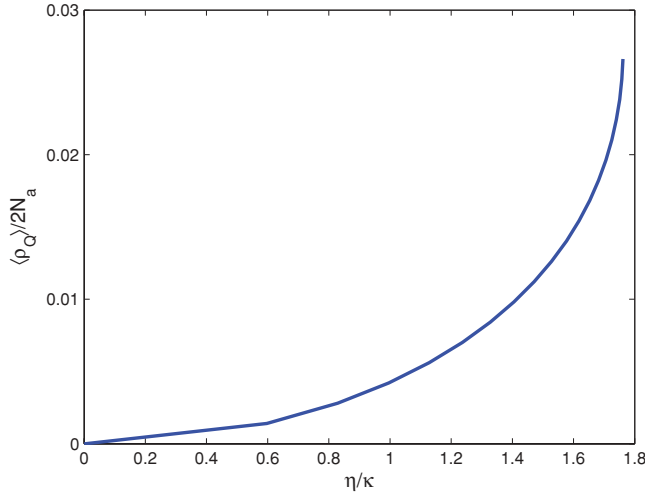


FIG. 3. Steady-state density order parameter $\hat{\rho}_Q$ (scaled with lattice number) vs the cavity-pumping strength η in the lower bistable branch of Fig. 2(b).

To gain more insight into the DW steady state, we introduce the natural density operator $\hat{\rho}_Q = \sum_k \hat{f}_{k+Q}^\dagger \hat{f}_k$ to characterize this state, which is given by

$$\langle \hat{\rho}_Q \rangle_{\text{DW}} = \sum_k \frac{\Delta_g}{\sqrt{\varepsilon_k^2 + \Delta_g^2}}. \quad (10)$$

From the above equation, we see that the density order $\langle \hat{\rho}_Q \rangle_{\text{DW}}$ follows the gap Δ_g . We solve Eq. (9) numerically and find that the gap Δ_g approaches zero continuously with vanishing pumping strength. Then, by Eq. (10), we give the curve of the steady-state density order $\langle \hat{\rho}_Q \rangle_{\text{DW}}$ (scaled with lattice number) versus pumping strength η in Fig. 3, where we find that the density order $\langle \hat{\rho}_Q \rangle_{\text{DW}}$ also approaches zero continuously at $\eta = 0$. This indicates a continuous transition from a free Fermi gas to a DW state occurring at vanishing pumping strength. This cavity-field-driven DW transition bears some similarity to the atomic self-organization transition in a transversally pumped atom-cavity system [18], where the atoms are also trapped and scattered by a superlattice potential (although of a quantum nature) and form a regular pattern when the cavity pumping is above a threshold value η_{cr} . However, there are still some distinctions between these two cases. First, the statistics of involved particles (bosons or fermions) are different: in our case, a free Fermi gas forms a DW state; while in Refs. [14, 18], a BEC transitions to a self-organized state of bosons. Second, as pointed out in Ref. [18], the self-organized state can be mapped to an incompressible Mott-like state; while in our case, the DW state is a compressible state, except at the specific filling of $\nu = 1/2$ where the chemical potential μ is in the gap.

B. Time evolution: Coherent oscillation

Now, we turn to the dynamical evolution in this coupled atom-cavity system. We integrate Eq. (4) numerically with constant pumping strength η . The initial atomic state is naturally chosen as the ground state of free Fermi gas (assuming $T = 0$): $\hat{\Psi}_{\text{init}} = \prod_k^{k_F} \hat{f}_k^\dagger |0\rangle$, where $|0\rangle$ is the vacuum

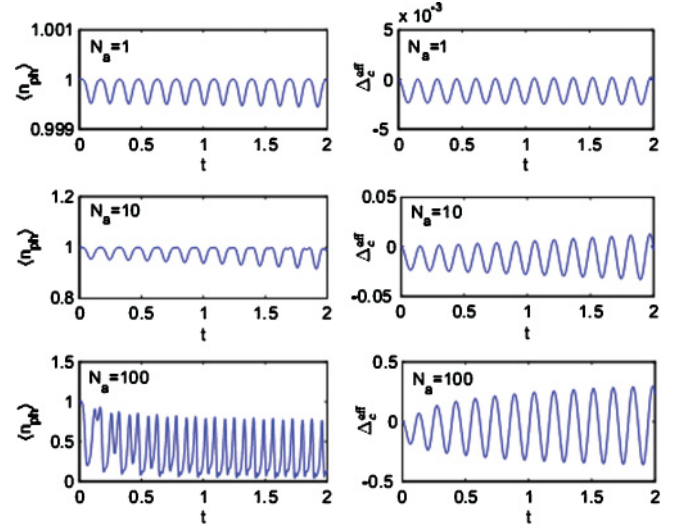


FIG. 4. Evolution of cavity photon number $\langle \hat{n}_{\text{ph}} \rangle$ (left panels) and effective cavity detuning Δ_c^{eff} (MHz, right panels) with times t for different atom numbers $N_a = 1, 10, 100$, with corresponding filling $\nu = 0.0025, 0.025, 0.25$, respectively. Other parameters are the same as in Fig. 2 with $\eta/\kappa = 1$.

state and k_F is the Fermi momentum. In Fig. 4, we give the numerical results of the mean cavity photon number $\langle \hat{n}_{\text{ph}} \rangle$ and effective cavity detuning δ_c versus times t for different atom numbers N_a , respectively.

From Fig. 4, we can easily observe a good periodical oscillation of the mean cavity photon number with time. To understand this, we consider the dynamical evolution process in detail. When the cavity is pumped by a driven laser with constant value at $t = 0$, the cavity field builds up in a short time of $1/\kappa$, which induces a transient-dipole potential on atoms in a far-detuning limit. Then the atoms are diffracted to a high-momentum state by this dynamical potential and shift the effective cavity detuning via $\Delta_c^{\text{eff}} = \Delta_c + \frac{U_0}{2} \sum_k \langle \hat{\sigma}_k^x \rangle$, which inversely changes the evolution of the cavity field. Note that the atomic motion can be seen as effective time-dependent oscillators, which can be obtained directly by differentiating the motion equation $d^2 \hat{\sigma}_k^y(t)/dt^2 = -(4\varepsilon_k^2 + U_0^2 \hat{n}^2) \hat{\sigma}_k^y(t)$. Because the time scale of the cavity damping ($1/\kappa$) is much faster than the motion of the effective oscillator, the cavity field can almost follow the mechanical motion adiabatically and give rise to the coherent oscillating behavior, which is a reflection of the atomic motion.

However, this kind of periodical oscillation of the mean cavity photon number becomes poor as the atom number increases. Actually, the effective mechanical oscillators of atomic motion are distinguishable and intimately relate to the atom number N_a . The oscillators will interfere with each other, with the effect determined by the frequency differences of these oscillators. With the increasing of the atom number, the frequency differences of these modes become remarkable and the good periodic behavior is damaged. This is the main difference compared to the previous work [7, 9], where actually only one effective mechanical mode couples to the cavity field, and the characteristic frequency only depends on the intrinsic many-body atomic state.

In addition, comparing the left and right panels of Fig. 4, we find that when the effective detuning crosses the resonance point $\Delta_c^{\text{eff}} = 0$, the cavity photon number does not reach the maximal value η^2/κ^2 . This is due to the retardation effect in which the cavity field cannot fully follow the change of the atomic state based on the parameters we have chosen.

So far we have limited this study to the cases of filling $\nu \leq 1/2$, however, similar dynamical analysis can be steadily extended to filling $\nu > 1/2$. It is worth noticing that from the normalization given by (5), some of the atomic motion ($\hat{n}_k + \hat{n}_{k+Q} = 2$, i.e., double occupied) is frozen and does not contribute to the dynamical evolution process up to a shift of cavity frequency scaled as N_a . In the limit case of $\nu = 1$, the Fermi atoms form a band insulator with all the effective degrees of freedom frozen for a sufficiently small pumping rate. The atoms only shift the cavity resonance with a constant value of $\frac{1}{2}U_0N_a$, and the dynamics of the cavity field with the atoms is decoupled.

IV. EXPERIMENTAL DISCUSSION

Finally, we design an experiment to investigate the dynamics of a degenerate Fermi gas in a 1D optical lattice inside a cavity. We choose the cavity length $L \sim 100 \mu\text{m}$, the cavity mode $\lambda_c \sim 500 \text{ nm}$, and several hundred cold atoms. The experimental protocol can be taken as follows: the ultracold Fermi atoms (such as ${}^6\text{Li}$, ${}^{86}\text{Rb}$) are first loaded into a quasi-1D optical-lattice potential inside a high-finesse optical cavity, with the traverse degrees of freedom confined by a strong (magnetic or optical) trapping potential. Then by cooling the system to the degenerate temperature, the fermions are expected to occupy the lowest Bloch band with the filling factor satisfying $\nu \leq 1$. By applying a pumping laser along the axis, the Fermi atoms suffer a dynamical instability and a

DW state may appear, which can be detected by optical Bragg scattering [23].

Generally, there are two methods to implement the pumping laser. The first is to slowly (adiabatically) vary the pumping strength to a given value, then the collective atomic state can follow the pumping field and a steady value of cavity photon is reached, unless it approaches the bistable regime where the adiabatic continuity breaks down, as shown by the dashed line in Fig. 2. The second is to turn on the pumping laser with a finite strength, which remains constant for a typical time t_o . The time evolution is described by the Heisenberg equations with the results given by Fig. 4.

V. CONCLUSION

In summary, we theoretically investigate the dynamics of a 1D-lattice degenerate Fermi gas coupled to a cavity field. In the off-resonance limit, the quantized-dipole potential induced by the cavity mode scatters the atoms into a DW state, which is interdependent with the intracavity-field potential. The optical bistability is found in the steady state for this atom-cavity system. Further, the dynamical evolution study shows that the cavity photon number exhibits the coherent oscillating behavior. We also propose an experimental protocol to observe these phenomena. Our research may benefit the study of the cavity QED with cold atoms and deepen the understanding of the cavity effect on atomic assemblies.

ACKNOWLEDGMENTS

This work is supported by the NSFC under Grants No. 10934010 and No. 60978019, as well as by the NKBRSCF under Grants No. 2010CB922904 and No. 2011CB921500. A.C.J. is supported by the NSFC under Grant No. 11704175.

-
- [1] F. Brennecke, T. Donner, S. Ritter, T. Bourdel, M. Köhn, and T. Esslinger, *Nature (London)* **450**, 268 (2007).
 - [2] Y. Colombe, T. Steinmetz, G. Dubois, F. Linke, D. Hunger, and J. Reichel, *Nature (London)* **450**, 272 (2007); P. Treutlein, D. Hunger, S. Camerer, T. W. Hänsch, and J. Reichel, *Phys. Rev. Lett.* **99**, 140403 (2007).
 - [3] I. B. Mekhov, C. Maschler, and H. Ritsch, *Nature Phys.* **3**, 319 (2007); *Phys. Rev. A* **76**, 053618 (2007).
 - [4] W. Chen, D. Meiser, and P. Meystre, *Phys. Rev. A* **75**, 023812 (2007); W. Chen and P. Meystre, *ibid.* **79**, 043801 (2009).
 - [5] C. Maschler and H. Ritsch, *Phys. Rev. Lett.* **95**, 260401 (2005); C. Maschler, I. B. Mekhov, and H. Ritsch, *Eur. Phys. J. D* **46**, 545 (2008).
 - [6] J. Larson, B. Damski, G. Morigi, and M. Lewenstein, *Phys. Rev. Lett.* **100**, 050401 (2008); J. Larson, S. Fernández-Vidal, G. Morigi, and M. Lewenstein, *New J. Phys.* **10**, 045002 (2008); J. Larson, G. Morigi, and M. Lewenstein, *Phys. Rev. A* **78**, 023815 (2008).
 - [7] F. Brennecke, S. Ritter, T. Donner, and T. Esslinger, *Science* **322**, 235 (2008).
 - [8] S. Gupta, K. L. Moore, K. W. Murch, and D. M. Stamper-Kurn, *Phys. Rev. Lett.* **99**, 213601 (2007); K. W. Murch, K. L. Moore, S. Gupta, and D. M. Stamper-Kurn, *Nature Phys.* **4**, 561 (2008).
 - [9] R. Kanamoto and P. Meystre, *Phys. Rev. Lett.* **104**, 063601 (2010).
 - [10] B. Nagorny, T. Elsässer, and A. Hemmerich, *Phys. Rev. Lett.* **91**, 153003 (2003); D. Kruse, C. von Cube, C. Zimmermann, and Ph. W. Courteille, *ibid.* **91**, 183601 (2003).
 - [11] J. M. Zhang, F. C. Cui, D. L. Zhou, and W. M. Liu, *Phys. Rev. A* **79**, 033401 (2009).
 - [12] K. Zhang, W. Chen, M. Bhattacharya, and P. Meystre, *Phys. Rev. A* **81**, 013802 (2010); W. Chen, D. S. Goldbaum, M. Bhattacharya, and P. Meystre, *ibid.* **81**, 053833 (2010).
 - [13] G. Szirmai, D. Nagy, and P. Domokos, *Phys. Rev. Lett.* **102**, 080401 (2009).
 - [14] P. Domokos and H. Ritsch, *Phys. Rev. Lett.* **89**, 253003 (2002); J. K. Asbóth, P. Domokos, H. Ritsch, and A. Vukics, *Phys. Rev. A* **72**, 053417 (2005).
 - [15] K. Baumann, C. Guerlin, F. Brennecke, and T. Esslinger, *Nature (London)* **464**, 1301 (2010).

- [16] D. Nagy, G. Kónya, G. Szirmai, and P. Domokos, *Phys. Rev. Lett.* **104**, 130401 (2010).
- [17] J. Keeling, M. J. Bhaseen, and B. D. Simons, *Phys. Rev. Lett.* **105**, 043001 (2010).
- [18] S. Fernández-Vidal, G. DeChiara, J. Larson, and Giovanna Morigi, *Phys. Rev. A* **81**, 043407 (2010).
- [19] A. Dorsel, J. D. McCullen, P. Meystre, E. Vignes, and H. Walther, *Phys. Rev. Lett.* **51**, 1550 (1983).
- [20] J. A. Sauer, K. M. Fortier, M. S. Chang, C. D. Hamley, and M. S. Chapman, *Phys. Rev. A* **69**, 051804 (2004).
- [21] L. Zhou, H. Pu, H. Y. Ling, and W. Zhang, *Phys. Rev. Lett.* **103**, 160403 (2009).
- [22] M. Lewenstein, A. Sanpera, V. Ahufinger, B. Damski, A. Sen, and U. Sen, *Adv. Phys.* **56**, 243 (2007).
- [23] S. Slama, C. von Cube, B. Deh, A. Ludewig, C. Zimmermann, and Ph. W. Courteille, *Phys. Rev. Lett.* **94**, 193901 (2005).